Electron microscopy

Whole larvae (day 5) were anaesthetized with 0.02% MESAB (3-aminobenzoic acid ethyl ester) and then fixed by immersion in 2.0% glutaraldehyde and 1.0% paraformaldehyde in normal solution (containing (in mM): 145 NaCl, 3 KCl, 1.8 $CaCl_2$, 10 HEPES, pH 7.2) overnight to several days at 4 °C. Specimens were fixed with 1.0% OsO_4 in H_2O for 10 min on ice, followed by fixation and contrast with 1.0% uranyl acetate for 1 h on ice, and then dehydrated with several steps in ethanol and embedded in Epon. Ultrathin sections (90–120 nm) of mutant *sputnik* and wild-type sibling anterior maculae were stained with lead citrate and uranyl acetate. Mutant bundles were serially sectioned at intervals of 1–2 μm or greater; both anterior maculae were present on each section. Wild-type bundles were partially sectioned (0.2–0.6 μm). Cross-sections of bundles contained up to five stereociliary tips (see Supplementary Fig. 2).

Received 12 December 2003; accepted 10 March 2004; doi:10.1038/nature02484.
Published online 31 March 2004.

1. Howard, J. & Hudspeth, A. J. Compliance of the hair bundle associated with gating of mechanoelectrical transduction channels in the bullfrog's saccular hair cell. *Neuron* **3,** 189–199 (1988).
2. Granato, M. *et al.* Genes controlling and mediating locomotion behavior of the zebrafish embryo and larva. *Development* **123,** 399–413 (1996).
3. Nicolson, T. *et al.* Genetic analysis of vertebrate sensory hair cell mechanosensation: the zebrafish circler mutants. *Neuron* **20,** 271–283 (1998).
4. Seiler, C. & Nicolson, T. Defective calmodulin-dependent rapid apical endocytosis in zebrafish sensory hair cell mutants. *J. Neurobiol.* **41,** 424–434 (1999).
5. Bork, J. *et al.* Usher syndrome 1D and nonsyndromic autosomal recessive deafness DFNB12 are caused by allelic mutations of the novel cadherin-like gene CDH23. *Am. J. Genet.* **68,** 26–37 (2000).
6. Bolz, H. *et al.* Mutation of *CDH23*, encoding a new member of the cadherin gene family, causes Usher syndrome type 1D. *Nature Genet.* **27,** 108–112 (2001).
7. Di Palma, F. *et al.* Mutations in *Cdh23*, encoding a new type of cadherin, cause stereocilia disorganization in *waltzer*, the mouse model for Usher syndrome type 1D. *Nature Genet.* **27,** 103–107 (2001).
8. Wilson, S. *et al.* Mutations in Cdh23 cause nonsyndromic hearing loss in waltzer mice. *Genomics* **74,** 228–233 (2001).
9. Wada, T. *et al.* A point mutation in a cadherin gene, Cdh23, causes deafness in a novel mutant, waltzer mouse niigata. *Biochem. Biophys. Res. Comm.* **283,** 113–117 (2001).
10. Siemens, J. *et al.* The Usher syndrome proteins cadherin 23 and harmonin form a complex by means of PDZ-domain interactions. *Proc. Natl Acad. Sci. USA* **99,** 14946–14951 (2002).
11. Boeda, B. *et al.* Myosin VIIa, harmonin and cadherin 23, three Usher I gene products that cooperate to shape the sensory hair cell bundle. *EMBO J.* **21,** 6689–6699 (2002).
12. Pickles, J. *et al.* The organization of tip links and stereocilia on hair cells of bird and lizard basilar papillae. *Hear. Res.* **41,** 31–42 (1989).
13. Goodyear, R. & Richardson, G. Distribution of the 275 kD hair cell antigen and cell surface specializations on auditory and vestibular hair bundles in the chicken inner ear. *J. Comp. Neurol.* **325,** 243–256 (1992).
14. Katori, Y., Tonosaki, A. & Takasaka, T. WGA lectin binding sites of the apical surface of corti epithelium: enhancement by back-scattered electron imaging in guinea-pig inner ear. *J. Elec. Microsc.* **45,** 207–212 (1996).
15. Goodyear, R. & Richardson, G. The ankle-link antigen: an epitope sensitive to calcium chelation associated with the hair-cell surface and the calycal processes of photoreceptors. *J. Neurosci.* **19,** 3761–3772 (1999).
16. Goodyear, R. J. & Richardson, G. P. A novel antigen sensitive to calcium chelation that is associated with the tip links and kinocilial links of sensory hair bundles. *J. Neurosci.* **23,** 4878–4887 (2003).
17. Goodyear, R. J. *et al.* A receptor-like inositol lipid phosphatase is required for the maturation of developing cochlear hair bundles. *J. Neurosci.* **23,** 9208–9219 (2003).
18. Pickles, J. & Corey, D. Mechanoelectrical transduction by hair cells. *Trends Neurosci.* **15,** 254–259 (1992).
19. Steel, K. & Kros, C. A genetic approach to understanding auditory function. *Nature Genet.* **27,** 143–149 (2001).
20. Ernest, S. *et al. Mariner* is defective in *myosin VIIA*: a zebrafish model for human hereditary deafness. *Hum. Mol. Genet.* **9,** 2189–2196 (2000).
21. Riley, B. B., Zhu, C., Janetopoulos, C. & Aufderheide, K. J. A critical period of ear development controlled by distinct populations of ciliated cells in the zebrafish. *Dev. Biol.* **191,** 191–201 (1997).
22. Siemens, J. *et al.* Cadherin 23 is a component of the tip link in hair cell stereocilia. *Nature* advance online publication 31 March 2004 (doi:10.1038/nature02483).
23. Neugebauer, D. & Thurm, U. Surface charges of the membrane and cell adhesion substances determine the structural integrity of hair bundles from the inner ear of fish. *Cell Tissue Res.* **249,** 199–207 (1987).
24. Leckband, D. & Sivasankar, S. Mechanism of homophilic cadherin adhesion. *Curr. Opin. Cell Biol.* **12,** 587–592 (2000).
25. Assad, J., Shepherd, G. & Corey, D. Tip-link integrity and mechanical transduction in vertebrate hair cells. *Neuron* **7,** 987–994 (1991).
26. Kachar, B., Parakkal, M., Kurc, M., Zhao, Y. & Gillespie, P. High-resolution structure of hair cell tip links. *Proc. Natl Acad. Sci. USA* **97,** 13336–13341 (2000).
27. Baumgartner, W. *et al.* Cadherin interaction probed by atomic force microscopy. *Proc. Natl Acad. Sci. USA* **97,** 4005–4010 (2000).
28. Sivasankar, S., Gumbiner, B. & Leckband, D. Direct measurements of multiple adhesive alignments and unbinding trajectories between cadherin extracellular domains. *Biophys. J.* **80,** 1758–1768 (2001).
29. Sidi, S., Friedrich, R. & Nicolson, T. NompC TRP channel required for vertebrate sensory hair cell mechanotransduction. *Science* **301,** 96–99 (2003).
30. Fleischmann, R. D. *et al.* Whole-genome random sequencing and assembly of *Haemophilus influenzae*. *Science* **269,** 496–512 (1995).
31. Westerfield, M. *The Zebrafish Book* 3rd edn (Univ. Oregon Press, Eugene, Oregon, 1995).

Supplementary Information accompanies the paper on **www.nature.com/nature**.

Acknowledgements We thank U. Schönberger, A. Hruscha and members of the electron microscopy laboratory (especially H. Schwarz) at the Max-Planck-Institut für Entwicklungsbiologie for their technical support and advice. This work was supported by funding from the SFB430 and DFG.

Competing interests statement The authors declare that they have no competing financial interests.

Correspondence and requests for materials should be addressed to T.N. (nicolson@ohsu.edu).
The sequence has been deposited in GenBank under accession number AY530192.

The Tübingen 2000 Screen Consortium: **F. van Bebber[1], E. Busch-Nentwich[1], R. Dahm[1], O. Frank[1], H.-G. Frohnhöfer[1], H. Geiger[1], D. Gilmour[1], S. Holley[1], J. Hooge[1], D. Jülich[1], H. Knaut[1], F. Maderspacher[1], H.-M. Maischein[1], C. Neumann[1], C. Nüsslein-Volhard[1], H. Roehl[1], U. Schönberger[1], C. Seiler[1], S. Sidi[1], M. Sonawane[1], A. Wehner[1], P. Erker[2], H. Habeck[2], U. Hagner[2], C. E. Hennen Kaps[2], A. Kirchner[2], T. Koblizek[2], U. Langheinrich[2], C. Loeschke[2], C. Metzger[2], R. Nordin[2], J. Odenthal[2], M. Pezzuti[2], K. Schlombs[2], J. deSantana-Stamm[2], T. Trowe[2], G. Vacun[2], B. Walderich[2], A. Walker[2] & C. Weiler[2]**

Affiliations for authors: 1, Max-Planck-Institut für Entwicklungsbiologie, Spemannstrasse 35, 72076 Tübingen, Germany; 2, Artemis Pharmaceuticals GmbH, 72076 Tübingen, Germany

Splicing of *oskar* RNA in the nucleus is coupled to its cytoplasmic localization

Olivier Hachet & Anne Ephrussi

European Molecular Biology Laboratory, Meyerhofstrasse 1, Postfach 10.2209, D-69117 Heidelberg, Germany

oskar **messenger RNA localization at the posterior pole of the** ***Drosophila*** **oocyte is essential for germline and abdomen formation in the future embryo[1,2]. The nuclear shuttling proteins Y14/Tsunagi and Mago nashi are required for** ***oskar*** **mRNA localization, and they co-localize with** ***oskar*** **mRNA at the posterior pole of the oocyte[3–5]. Their human homologues, Y14/RBM8 and Magoh, are core components of the exon–exon junction complex (EJC)[6–9]. The EJC is deposited on mRNAs in a splicing-dependent manner, 20–24 nucleotides upstream of exon–exon junctions, independently of the RNA sequence[6–8]. This indicates a possible role of splicing in** ***oskar*** **mRNA localization, challenging the established notion that the** ***oskar*** **3′ untranslated region (3′UTR) is sufficient for this process. Here we show that splicing at the first exon–exon junction of** ***oskar*** **RNA is essential for** ***oskar*** **mRNA localization at the posterior pole. We revisit the issue of sufficiency of the** ***oskar*** **3′UTR for posterior localization and show that the localization of unrelated transcripts bearing the** ***oskar*** **3′UTR is mediated by endogenous** ***oskar*** **mRNA. Our results reveal an important new function for splicing: regulation of messenger ribonucleoprotein complex assembly and organization for mRNA cytoplasmic localization.**

To address the requirement of splicing for *oskar* mRNA localization, we tested the effect of deleting *oskar* introns on mRNA localization by a transgenic approach. We evaluated *oskar* mRNA localization in the $osk^{A87}/Df(3R)p^{XT103}$ background, in which no endogenous *oskar* RNA is produced[10]. $osk^{A87}/Df(3R)p^{XT103}$ ovaries

undergo an early arrest of oogenesis that can be rescued by transgenic *oskar* mRNA (O.H., P. Závorsky, M. Erdélyi, A. Jenny and A.E., unpublished data), providing a phenotypic confirmation of efficient transgene expression. Because the only source of *oskar* mRNA in these experiments is transgenic, we refer to each genotype by the name of the *oskar* transgene.

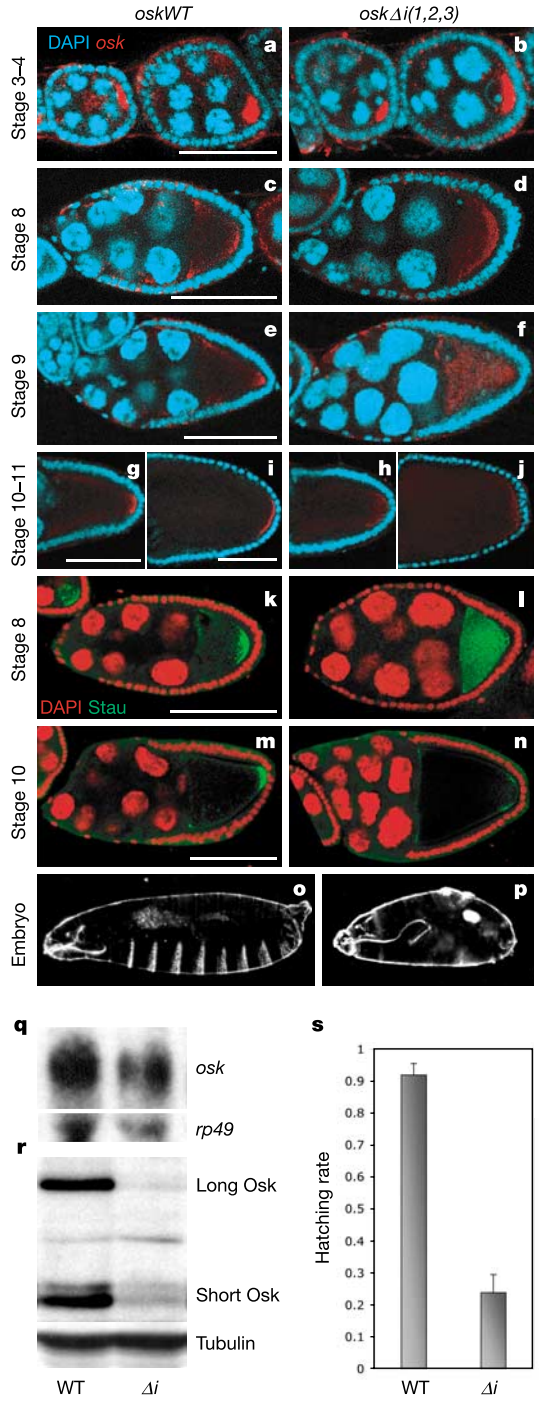

Figure 1 *oskar* mRNA produced from an intronless *oskar* gene fails to localize at the posterior of the oocyte. **a**–**p**, Left and right panels show *oskWT* and *oskΔi(1,2,3)* egg chambers, respectively. Scale bar, 100 μm. **a**–**j**, *oskar* mRNA detected by fluorescent *in situ* hybridization is shown in red; 4,6-diamidino-2-phenylindole (DAPI) staining is in blue. **k**–**n**, Staufen detected with a fluorescent antibody is shown in green; DAPI staining is in red. **o**, **p**, Cuticle preparation of embryos produced by *oskWT* and *oskΔi(1,2,3)* females. **q**, **r**, Northern and western blots detecting *oskar* mRNA (**q**) and Oskar protein (**r**) in ovarian extracts of *oskWT* (WT) and *oskΔi(1,2,3)* (*Δi*) females. *rp49* RNA and tubulin protein are loading controls. **s**, Hatching rate of embryos produced by *oskWT* (WT) and *oskΔi(1,2,3)* (*Δi*) females.

We first investigated the localization of *oskar* mRNA produced from the intronless transgene *oskΔi(1,2,3)*, in which the three *oskar* introns *i1*, *i2* and *i3* were deleted. During early oogenesis, *oskΔi(1,2,3)* mRNA is correctly transported from the nurse cells to the oocyte (Fig. 1a, b) indicating that *oskar* introns are dispensable both for nuclear export and the early phase of *oskar* mRNA transport. A defect in *oskΔi(1,2,3)* mRNA localization becomes evident during mid-oogenesis. At stage 8, *oskΔi(1,2,3)* mRNA distribution seems diffuse compared with *oskWT* mRNA (Fig. 1c, d). At stage 9, whereas *oskWT* mRNA accumulates at the posterior with a transient accumulation at the anterior corners[1,2], *oskΔi(1,2,3)* mRNA is distributed throughout the entire ooplasm (Fig. 1e, f). During late oogenesis, only a small amount of *oskΔi(1,2,3)* mRNA is detected in an extended posterior crescent, most probably reflecting local anchoring[11] of mRNA randomly distributed in the posterior area during mid-oogenesis (Fig. 1g–j). Consistent with the *oskΔi(1,2,3)* mRNA localization defect was our finding that Staufen protein, a marker for *oskar* mRNA, is similarly mislocalized (Fig. 1k–n). Although *oskar* mRNA levels are similar in *oskWT* and *oskΔi(1,2,3)* ovaries (Fig. 1q), *oskΔi(1,2,3)* mRNA is poorly translated, presumably reflecting the requirement of localization for *oskar* mRNA translation[12–14] (Fig. 1r). Finally, more than two-thirds of the embryos from eggs laid by *oskΔi(1,2,3)* females fail to hatch (Fig. 1s) and show a severe posterior group phenotype (Fig. 1o, p).

We next systematically deleted *oskar* introns to assess their relative contribution in *oskar* mRNA localization. The results show that, whereas the mRNAs produced from all *i1*-containing transgenes are localized (*oskWT*, *oskΔi(2,3)*, *oskΔi2* and *oskΔi3*), those produced from all *i1*-deleted transgenes are mislocalized, although they accumulate correctly in the oocyte (*oskΔi(1,2,3)*, *oskΔi(1,3)*, *oskΔi(1,2)* and *oskΔi1*) (Fig. 2a). The distributions of mRNAs produced from the *oskΔi(2,3)* transgene, containing only *i1*, and from the *oskΔi1* transgene, lacking only *i1*, are shown for comparison (Fig. 2b–e). Although the absence of *i2* and *i3* does not affect *oskΔi(2,3)* mRNA localization, *oskΔi1* mRNA fails to localize at the posterior pole of stage 9 and 10 oocytes, although *i2* and *i3* are correctly spliced (Supplementary Fig. S1). Confirming the previously reported *oskar* mRNA-dependent localization of Y14 (ref. 3), Y14 fails to localize in *oskΔi1* oocytes (Fig. 2f, g). The fact that *oskΔi(2,3)* mRNA supports Y14 localization to the posterior shows that splicing of *i1* is sufficient for the association of Y14 with *oskar* mRNA. Thus, our results reveal an unexpected and distinct role of *i1*, compared with *i2* and *i3*, in *oskar* mRNA localization. They indicate either that *i1* contains sequence-specific information or that splicing at the *i1* position is essential for *oskar* mRNA localization.

To discriminate between these two possibilities, we tested the localization of mRNAs produced by a transgene in which the *i1* sequence was replaced by *i3*, called *osk(i3 in i1)*. We found that *osk(i3 in i1)* mRNA localizes at the posterior, showing that, although *i3* is unable to promote *oskar* mRNA localization when located at its normal position, *i3* can functionally substitute for *i1* when placed in the *i1* context, between exons I and II (Fig. 3a, b). Consistent with this was our observation that the EJC component Y14 is recruited by *osk(i3 in i1)* mRNA, as revealed by the localization of Y14 at the posterior pole (Fig. 3c, d), indicating that Y14 recruitment is independent of intron sequence. This demonstrates the importance of splicing at the first exon–exon junction of *oskar* mRNA, rather than a specific requirement for *i1*, for *oskar* mRNA localization. These results show that *oskar* RNA splicing and localization are mechanistically coupled.

The demonstration that splicing is required for *oskar* mRNA localization seemingly contradicts previous work reporting that the *oskar* 3′UTR is sufficient for mRNA targeting to the posterior pole of the oocyte. This conclusion was based on several studies

of *lacZ–osk3′UTR* hybrid RNAs, in which the intronless *lacZ* gene was fused to the *oskar* 3′UTR and the chimaeric mRNAs were observed to localize at the oocyte posterior[15,16]. This apparent contradiction prompted us to revisit the role of the 3′UTR in *oskar* mRNA localization. We considered the possibility that the localization of *lacZ–osk3′UTR* mRNA might be influenced by endogenous *oskar* mRNA, which was present in all previous studies. A direct analysis of *lacZ–osk3′UTR* mRNA localization in *oskar* RNA-null oocytes is prevented by the early oogenesis arrest of the $osk^{A87}/Df(3R)p^{XT103}$ mutant. We therefore examined the localization of *lacZ–osk3′UTR* mRNAs in *oskWT* and *oskΔi(1,2,3)* oocytes, in which transgenic *oskar* mRNA supports oocyte development beyond the early stages. We found that although *lacZ–osk3′UTR* mRNA localizes correctly in *oskWT* oocytes, it fails to accumulate at the posterior pole of *oskΔi(1,2,3)* oocytes, as revealed by *lacZ in situ* hybridization (Fig. 4a, b). In addition, when placed in the Oskar protein-null background $osk^{84}/Df(3R)p^{XT103}$, in which the osk^{84} nonsense mRNA localizes correctly until stage 10 of oogenesis[1,2], *lacZ–osk3′UTR* mRNA also localizes at the posterior pole (Fig. 4c). Taken together, these results demonstrate that an endogenous source of *oskar* mRNA is required for *lacZ–osk3′UTR* localization at the posterior pole, and that this effect is independent of Oskar protein. Localization of the *lacZ–osk3′UTR* hybrid RNA to the posterior pole is therefore most probably due to its hitchhiking on endogenous *oskar* mRNA localization complexes, whose assembly involves splicing. Our results indicate that the *oskar* 3′UTR promotes association of the RNA into higher-order *oskar* messenger ribonucleoprotein (mRNP) complexes. This idea is consistent with estimates indicating that *oskar* mRNA particles contain about 100 *oskar* mRNA molecules[11]. The assembly of such multi-mRNP particles might be mediated by protein–protein interactions involving factors bound to the 3′UTR or by direct RNA–RNA interaction as occurs with *bicoid* mRNA[17,18].

Although the *oskar* 3′UTR and associated factors are clearly important for *oskar* mRNA localization, because *oskar* transcripts lacking the 3′UTR fail to localize[15], our data show that *oskar* mRNA localization requires additional factors recruited to the mRNA upon splicing. Thus, information imparted to *oskar* RNA in the nucleus during pre-mRNA processing is crucial for the localization of *oskar* mRNA at the posterior pole of the oocyte cytoplasm. The fact that both splicing and the EJC components Y14 and Mago nashi are essential for *oskar* mRNA localization[3–5] indicates that *oskar* RNA splicing and cytoplasmic localization are mechanistically coupled by the splicing-dependent deposition of the EJC. Unexpectedly, of the three *oskar* intron positions, only the first is strictly required and functional for *oskar* mRNA localization, although an EJC is presumably assembled at each *oskar* mRNA exon–exon junction. This indicates not only that an EJC landmark is required but also that its position is essential for *oskar* mRNA localization at the oocyte posterior. The importance of the splicing position, and thus of the EJC on *oskar* mRNA, suggests a structural role of the Y14–Mago nashi heterodimer[3–5], eIF4AIII[19] and Barentsz[19,20], in assembly of the *oskar* mRNA localization complex. The first EJC landmark on *oskar* mRNA might have a pivotal function in mediating interactions between factors bound to different regions of *oskar* mRNA, including the 5′ cap, the 3′UTR and potentially the coding region. We propose that the position of the first *oskar* EJC landmark is crucial in specifying the architecture of the *oskar* mRNA localization complex. This structural model could explain why the EJC is not always involved in cytoplasmic mRNA localization and why the transport of *gurken* and *bicoid* mRNAs, both of which are produced from intron-containing genes and are thus presumably imprinted with the EJC, seems to be independent of the EJC[3–5]. Our model also suggests that alternatively spliced mRNAs might be directed to different cytoplasmic locations, depending on the formation of alternative mRNP complex architectures.

In humans, EJC imprinting allows the recognition of premature termination codons, triggering mRNA degradation by activation of

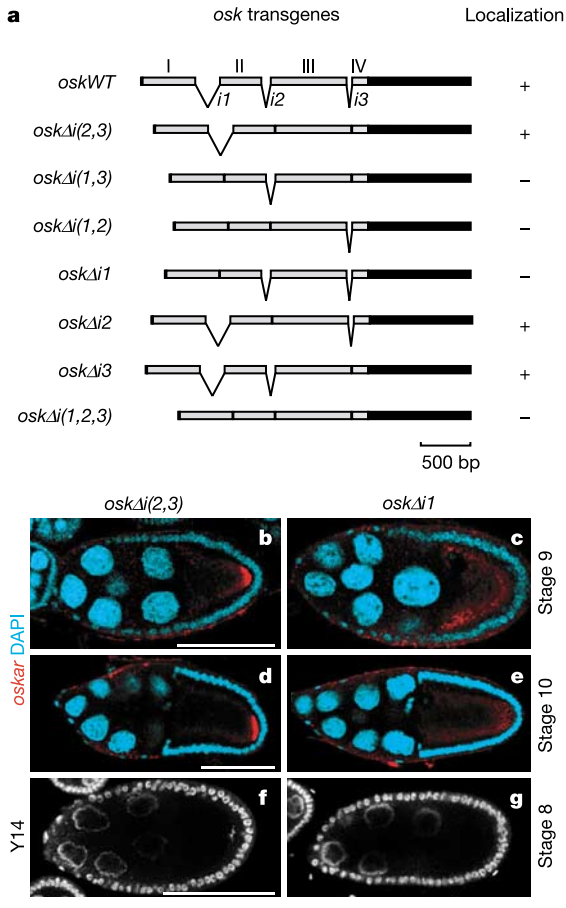

Figure 2 The first intron of *oskar* is required for *oskar* mRNA localization. **a**, Schematic representation of the different *oskar* transgenes. Black boxes represent 5′ and 3′ UTRs, grey boxes represent exons, and linkers represent introns. The capacity of the mRNA to localize is indicated in the right column. bp, base pairs. **b**–**g**, Left and right panels show *oskΔi(2,3)* and *oskΔi1* egg chambers, respectively. Scale bar, 100 μm. **b**, **e**, *oskar* mRNA fluorescent *in situ* hybridization is shown in red; 4,6-diamidino-2-phenylindole (DAPI) staining is in blue. **f**, **g**, Y14 fluorescent immunostaining.

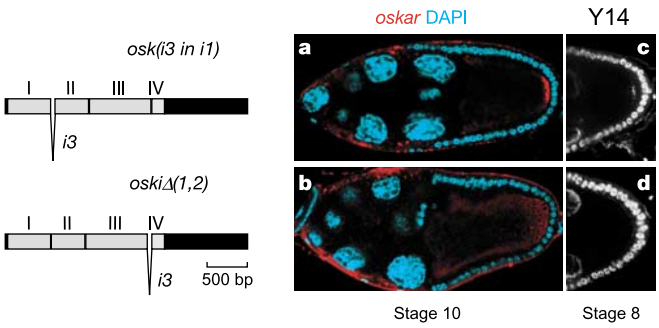

Figure 3 Splicing at the first exon–exon junction of *oskar* mRNA is essential for its localization at the posterior pole of the oocyte. **a**–**d**, Top and bottom panels show *osk(i3 in i1)* and *oskΔi(1,2)* egg chambers, respectively. bp, base pairs. **a**, **b**, *oskar* fluorescent *in situ* hybridization is shown in red; 4,6-diamidino-2-phenylindole (DAPI) staining is in blue. **c**, **d**, Y14 fluorescent immunostaining.

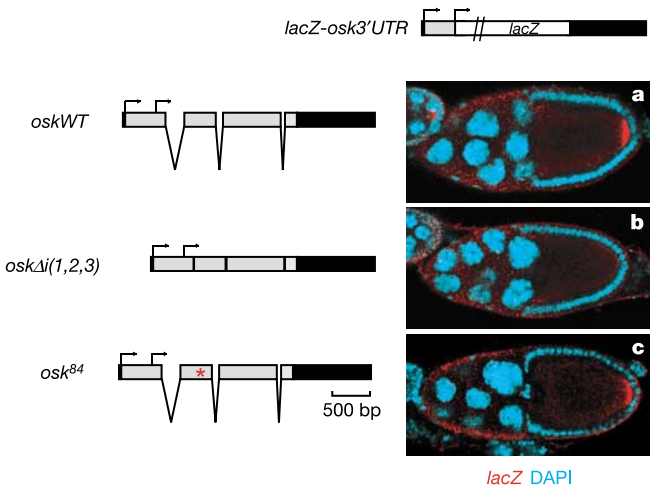

Figure 4 *lacZ–osk3′ UTR* mRNA localization at the posterior of the oocyte depends on endogenous *oskar* mRNA. **a**–**c**, *lacZ* fluorescent *in situ* hybridization is shown in red; 4,6-diamidino-2-phenylindole (DAPI) staining is in blue in *oskWT* (**a**), *oskΔi(1,2,3)* (**b**) and *osk*^{84}/*Df(3R)p*^{XT103} (**c**). Arrows represent the two *oskar* initiation codons[13] and the red star indicates the position of the nonsense mutation in the *osk*^{84} allele. bp, base pairs.

the nonsense-mediated decay (NMD) pathway. In *Drosophila*, however, although NMD factors and EJC components are conserved, the recognition of premature termination codons depends neither on the EJC nor on intron position[21]. The involvement of Y14, Magoh, eIF4AIII and Barentsz in NMD in humans[19,22,23] and in *oskar* mRNA localization in *Drosophila*[3–5,19,20] is striking and suggests the maintenance of an evolutionarily conserved complex with divergent functions. However, this does not exclude a possible involvement of splicing and the EJC in the cytoplasmic localization of some mRNAs in vertebrates. In particular, the localization of Barentsz in hippocampal neurons[24] suggests that the use of these factors in cytoplasmic mRNA localization has been conserved in vertebrates. It will be of particular interest to determine whether the transport of other localized mRNAs is dependent on the EJC and to evaluate the relevance of the conservation of the EJC regarding mRNA cytoplasmic localization. □

Methods

Transgene constructions

pUASp *oskWT* and pUASp *oskΔ(i1,i2,i3)* transgenes were constructed by cloning genomic and cDNA versions of *oskar* as *Bam*HI/*Pst*I fragments from pGem g.*osk*[1] and pGem g/c.*osk* (A.E., unpublished data), respectively, into pUASp Casper[25] digested with *Bam*HI/*Pst*I. To construct the different intron-deleted transgenes, genomic *oskar* was first subcloned into the small vector pSP72 to allow the subsequent use of *Msc*I and *Mlu*I unique restriction sites in *osk* exons II and III. pSP72 *oskWT* was prepared by subcloning the pGem g-osk *Bam*HI *Nsi*I-blunt-ended fragment into pSP72 *Bam*HI *Xho*I-blunt ended. pSP72 *oskΔi1*, pSP72 *oskΔi2* and pSP72 *oskΔi(1,2)* were then constructed by exchanging the *Bam*HI *Msc*I, *Msc*I *Mlu*I and *Bam*HI *Mlu*I fragments of pSP72 *oskWT* with their cDNA equivalents from pBlue *osk*[1]. All *pUASp osk* derivatives were constructed by cloning the appropriate *Bam*HI *Mlu*I fragment of pSP72 *oskΔi1*, *pSP72 oskΔi2*, pSP72 *oskΔi(1,2)* and pSP72 *oskWT* into the appropriate vector (pUASp *oskWT* or pUASp *oskΔi(1,2,3)*). For the pUASp *osk(i3 in i1)* transgene, an *(i3 in i1)* fragment was generated by using the splicing by overlap extension method[26] and cloned in pUASp *oskΔi(1,2,3)* with the use of *Bam*HI *Mlu*I restriction sites. Primer sequences are available from the authors on request.

Rescue experiments

Transgenic stocks were generated by germline-mediated transformation in the *w1118* background. Rescue of the *osk*^{A87}/*Df(3R)p*^{XT103} oogenesis phenotype by *oskar* transgenes was performed by driving their expression by using both Nanos-Gal4:VP16 and pCOG-Gal4:VP16. In the case of the *lacZ* experiment, only the Nanos-Gal4:VP16 driver was used, at 29 °C. For the equivalent production of *oskar* mRNA from the *oskWT* and *oskΔi(1,2,3)* transgenes, the flies were raised at 21 and 25 °C, respectively. In all other experiments, flies were raised at 21 °C. For each *oskar* transgene, more than 50 stage-9 to stage-10 egg chambers were analysed for both *oskar* mRNA and Staufen localization.

RNA and protein analysis

Flies were raised at the appropriate temperature for 4 days, allowed to lay eggs for 1 day to evaluate the hatching rate of the progeny, then dissected. For RNA analysis, ovaries were homogenized with a pestle in Trizol (Invitrogen) and processed according to the manufacturer's instructions. Each lane corresponds to 20 ovaries. Northern blotting was performed as described[27]. Radioactive DNA probes were synthesized from a *Sac*I fragment of pBlue *osk* and an *Xho*I *Bam*HI fragment of pBS RP49, with the High Prime kit (Roche). For protein analysis, ovaries were homogenized with a pestle in 2× SDS–polyacrylamide gel electrophoresis (SDS–PAGE) sample buffer, and analysed by 10% SDS–PAGE. Each lane corresponds to two ovaries. Western blotting was performed as described[28].

Whole-mount *in situ* staining

Staufen fluorescent immunostaining was performed as described[3]. For fluorescent *in situ* hybridization, ovaries were fixed with 4% formaldehyde in PBS for 30 min, then treated as described[29].

Splicing assay

RNA extracted from *oskΔi1* ovaries were subjected to polymerase chain reaction (PCR) with reverse transcription by using primers hybridizing to exon I and exon III sequences for the intron 2 splicing assay, and primers hybridizing to exon III and exon IV (in the 3′ UTR) for the intron 3 splicing assay. The DNA fragments were then amplified by PCR with primers allowing the discrimination of spliced from unspliced versions of the RNA, based on the size of the amplified fragment. The sequence of the primers used in this assay is available from the authors on request.

Fly stocks

The following fly stocks were used: *osk*^{84} (ref. 29), *osk*^{A87} (ref. 10), *Df(3R)p*^{XT103} (ref. 30), Nanos-Gal4:VP16 (ref. 25), pCog-Gal4:VP16 (ref. 25) and *lacZ–osk3′ UTR* (ref. 16).

Received 19 December 2003; accepted 23 March 2004; doi:10.1038/nature02521.

1. Ephrussi, A., Dickinson, L. K. & Lehmann, R. Oskar organizes the germ plasm and directs localization of the posterior determinant *nanos*. *Cell* **66,** 37–50 (1991).
2. Kim-Ha, J., Smith, J. L. & Macdonald, P. M. *oskar* mRNA is localized to the posterior pole of the *Drosophila* oocyte. *Cell* **66,** 23–35 (1991).
3. Hachet, O. & Ephrussi, A. *Drosophila* Y14 shuttles to the posterior of the oocyte and is required for *oskar* mRNA transport. *Curr. Biol.* **11,** 1666–1674 (2001).
4. Mohr, S. E., Dillon, S. T. & Boswell, R. E. The RNA-binding protein Tsunagi interacts with Mago Nashi to establish polarity and localize *oskar* mRNA during *Drosophila* oogenesis. *Genes Dev.* **15,** 2886–2899 (2001).
5. Newmark, P. A. & Boswell, R. E. The *mago nashi* locus encodes an essential product required for germ plasm assembly in *Drosophila*. *Development* **120,** 1303–1313 (1994).
6. Kataoka, N., Diem, M. D., Kim, V. N., Yong, J. & Dreyfuss, G. Magoh, a human homolog of *Drosophila* mago nashi protein, is a component of the splicing-dependent exon–exon junction complex. *EMBO J.* **20,** 6424–6433 (2001).
7. Le Hir, H., Izaurralde, E., Maquat, L. E. & Moore, M. J. The spliceosome deposits multiple proteins 20–24 nucleotides upstream of mRNA exon–exon junctions. *EMBO J.* **19,** 6860–6869 (2000).
8. Kim, V. N. *et al.* The Y14 protein communicates to the cytoplasm the position of exon–exon junctions. *EMBO J.* **20,** 2062–2068 (2001).
9. Le Hir, H., Gatfield, D., Braun, I. C., Forler, D. & Izaurralde, E. The protein Mago provides a link between splicing and mRNA localization. *EMBO Rep.* **2,** 1119–1124 (2001).
10. Vanzo, N. F. & Ephrussi, A. Oskar anchoring restricts pole plasm formation to the posterior of the *Drosophila* oocyte. *Development* **129,** 3705–3714 (2002).
11. Glotzer, J. B., Saffrich, R., Glotzer, M. & Ephrussi, A. Cytoplasmic flows localize injected *oskar* RNA in *Drosophila* oocytes. *Curr. Biol.* **7,** 326–337 (1997).
12. Rongo, C., Gavis, E. R. & Lehmann, R. Localization of *oskar* RNA regulates *oskar* translation and requires Oskar protein. *Development* **121,** 2737–2746 (1995).
13. Markussen, F. H., Michon, A. M., Breitwieser, W. & Ephrussi, A. Translational control of *oskar* generates short OSK, the isoform that induces pole plasma assembly. *Development* **121,** 3723–3732 (1995).
14. Kim-Ha, J., Kerr, K. & Macdonald, P. M. Translational regulation of *oskar* mRNA by bruno, an ovarian RNA-binding protein, is essential. *Cell* **81,** 403–412 (1995).
15. Kim-Ha, J., Webster, P. J., Smith, J. L. & Macdonald, P. M. Multiple RNA regulatory elements mediate distinct steps in localization of *oskar* mRNA. *Development* **119,** 169–178 (1993).
16. Gunkel, N., Yano, T., Markussen, F. H., Olsen, L. C. & Ephrussi, A. Localization-dependent translation requires a functional interaction between the 5′ and 3′ ends of *oskar* mRNA. *Genes Dev.* **12,** 1652–1664 (1998).
17. Ferrandon, D., Koch, I., Westhof, E. & Nusslein-Volhard, C. RNA-RNA interaction is required for the formation of specific *bicoid* mRNA 3′ UTR-STAUFEN ribonucleoprotein particles. *EMBO J.* **16,** 1751–1758 (1997).
18. Wagner, C. *et al.* Dimerization of the 3′UTR of *bicoid* mRNA involves a two-step mechanism. *J. Mol. Biol.* **313,** 511–524 (2001).
19. Palacios, I., Gatfield, D., St Johnston, D. & Izaurralde, E. An eIF4AIII-containing complex required for mRNA localization and non-sense-mediated decay. *Nature* **427,** 753–757 (2004).
20. van Eeden, F. J., Palacios, I. M., Petronczki, M., Weston, M. J. & St Johnston, D. Barentsz is essential for the posterior localization of *oskar* mRNA and colocalizes with it to the posterior pole. *J. Cell Biol.* **154,** 511–524 (2001).
21. Gatfield, D., Unterholzner, L., Ciccarelli, F. D., Bork, P. & Izaurralde, E. Nonsense-mediated mRNA decay in *Drosophila*: at the intersection of the yeast and mammalian pathways. *EMBO J.* **22,** 3960–3970 (2003).
22. Fribourg, S., Gatfield, D., Izaurralde, E. & Conti, E. A novel mode of RBD-protein recognition in the Y14–Mago complex. *Nature Struct. Biol.* **10,** 433–439 (2003).

23. Gehring, N. H., Neu-Yilik, G., Schell, T., Hentze, M. W. & Kulozik, A. E. Y14 and hUpf3b form an NMD-activating complex. *Mol. Cell* **11,** 939–949 (2003).
24. Macchi, P. *et al.* Barentsz, a new component of the Staufen-containing ribonucleoprotein particles in mammalian cells, interacts with Staufen in an RNA-dependent manner. *J. Neurosci.* **23,** 5778–5788 (2003).
25. Rørth, P. Gal4 in the *Drosophila* female germline. *Mech. Dev.* **78,** 113–118 (1998).
26. Horton, R. M., Cai, Z. L., Ho, S. N. & Pease, L. R. Gene splicing by overlap extension: tailor-made genes using the polymerase chain reaction. *Biotechniques* **5,** 528–535 (1991).
27. Ausubel, F. M. *et al.* (eds) *Current Protocols in Molecular Biology* vol. 1 (Wiley, New York, 1997).
28. Riechmann, V., Gutierrez, G. J., Filardo, P., Nebreda, A. R. & Ephrussi, A. Par-1 regulates stability of the posterior determinant Oskar by phosphorylation. *Nature Cell Biol.* **4,** 337–342 (2002).
29. Wilkie, G. S., Shermoen, A. W., O'Farrell, P. H. & Davis, I. Transcribed genes are localized according to chromosomal position within polarized *Drosophila* embryonic nuclei. *Curr. Biol.* **9,** 1263–1266 (1999).
30. Lehmann, R. & Nusslein-Volhard, C. Abdominal segmentation, pole cell formation, and embryonic polarity require the localized activity of *oskar*, a maternal gene in *Drosophila*. *Cell* **47,** 141–152 (1986).

Supplementary Information accompanies the paper on **www.nature.com/nature**.

Acknowledgements We thank A.-M. Voie for embryo injections for transgenesis, S. Curado for the *osk*^{A87}, Nanos-Gal4:VP16 recombinant stock, A. Cyrklaff for the *oskar in situ* probe, P. Rørth for the pCog-Gal4:VP16 driver, D. St Johnston for anti-Staufen antibody, and members of the Ephrussi laboratory, V. Hachet and E. Izaurralde for advice and comments on the manuscript. O.H. was supported in part by a predoctoral 'allocation de recherche' from the French government.

Competing interests statement The authors declare that they have no competing financial interests.

Correspondence and requests for materials should be addressed to A.E. (ephrussi@embl-heidelberg.de).

erratum

Enzymic activation and transfer of fatty acids as acyl-adenylates in mycobacteria

Omita A. Trivedi, Pooja Arora, Vijayalakshmi Sridharan, Rashmi Tickoo, Debasisa Mohanty & Rajesh S. Gokhale

Nature **428,** 441–445 (2004).

In this Letter to *Nature*, lanes FadD17, -19, and -28 of Fig. 1a did not appear. Figure 1a should have appeared as shown. □

a